

1Q1

2

3

4

5

6

7

8

9

10

11

12

13

14

15Q2

16

17

18

19

20

21

22

23

24

25

26

27

28

29

30

31

32

33

34

35

36

37

38

39

40

41

42

43

44

45

46

47

48

49

50

51

52

53

54

55

56

57

58

59

60

61

62

63

64

65

66



ELSEVIER

Contents lists available at ScienceDirect

Earth and Planetary Science Letters

www.elsevier.com/locate/epsl



Hydrologically induced slope deformations detected by GPS and clinometric surveys in the Cansiglio Plateau, southern Alps

R. Devoti^{a,*}, D. Zuliani^b, C. Braitenberg^c, P. Fabris^b, B. Grillo^c

^a Centro Nazionale Terremoti, Istituto Nazionale di Geofisica e Vulcanologia, Roma, Italy

^b Centro Ricerche Sismologiche, Istituto Nazionale di Oceanografia e di Geofisica Sperimentale, Udine, Italy

^c Department of Mathematics and Geosciences, University of Trieste, Italy

ARTICLE INFO

Article history:

Received 22 August 2014

Received in revised form 6 March 2015

Accepted 9 March 2015

Available online xxx

Editor: P. Shearer

Keywords:

Geodesy

GPS surface deformation

Karst hydrogeology

ABSTRACT

Changes in groundwater or surface water level may cause observable deformation of the drainage basins in different ways. We describe an active slope deformation monitored with GPS and tiltmeter stations in a karstic limestone plateau in southeastern Alps (Cansiglio Plateau). The observed transient GPS deformation clearly correlates with the rainfall. Both GPS and tiltmeter equipments react instantly to heavy rains displaying abrupt offsets, but with different time constants, demonstrating the response to different catchment volumes. The GPS movement is mostly confined in the horizontal plane (SSW direction) showing a systematic tendency to rebound in the weeks following the rain. Four GPS stations concur to define a coherent deformation pattern of a wide area ($12 \times 5 \text{ km}^2$), concerning the whole southeastern slope of the plateau. The plateau expands and rebounds radially after rain by an amount up to a few centimeters and causing only small vertical deformation. The effect is largest where karstic features are mostly developed, at the margin of the plateau where a thick succession of Cretaceous peritidal carbonates faces the Venetian lowland. A couple of tiltmeters installed in a cave at the top of the plateau, detect a much faster deformation, that has the tendency to rebound in less than 6 h. The correlation to rainfall is less straightforward, and shows a more complex behavior during rainy weather. The different responses demonstrate a fast hydrologic flow in the more permeable epikarst for the tiltmeters, drained by open fractures and fissures in the neighborhood of the cave, and a rapid tensile dislocation of the bedrock measured at the GPS stations that affect the whole slope of the mountain. In the days following the rain, both tiltmeter and GPS data show a tendency to retrieve the displacement which is consistent with the phreatic discharge curve. We propose that hydrologically active fractures recharged by rainfall are the most likely features capable to induce the observed strain variations.

© 2015 Elsevier B.V. All rights reserved.

1. Introduction

In the last decade, surface deformation attributed to hydrological processes has been observed with InSAR and GPS techniques in different aquifer systems. A number of papers reported measurable effects in response to groundwater level changes in different geographical areas (Bawden et al., 2001; Lanari et al., 2004; Argus et al., 2005). The San Gabriel Valley basin (Los Angeles, California) experienced an expansion of about 1 cm and an uplift of nearly 5 cm due to a heavy rainfall during winter 2004–2005 (King et al., 2007; Ji and Herring, 2012). Recently Diaz et al. (2014) detected an unusual spectral signature in seismic data, recorded

also as local strain variations, that were related to the discharge of the Aragon River in the southern Pyrenees (Spain). Rainfall and snowmelt episodes were identified to cause distinctive signatures in the seismic and strain measurements throughout the discharge phase in porous and fractured media.

Also tilt measurements have been long known to be affected by various hydrologic processes at the level of few micro-radians (μrad). One of the first works in Italy that claim for “micro-movements” caused by local rainfall was carried out by Caloi and Migani (1972), in which a couple of clinographs revealed a tilt towards SSE in correspondence of rain, in an area not far from our study region (70 km NE of the Cansiglio Plateau). The hydrologic induced deformation could also be linked to the seasonal modulation of the regional shallow seismicity in the southeastern Alps (Braitenberg, 2000).

Similar studies in different environments revealed the effect of groundwater on tiltmeter measurements (e.g. Edge et al., 1981;

* Corresponding author at: Centro Nazionale Terremoti, Istituto Nazionale di Geofisica e Vulcanologia, Via di Vigna Murata 605, 00143 Roma, Italy.

E-mail address: roberto.devoti@ingv.it (R. Devoti).

<http://dx.doi.org/10.1016/j.epsl.2015.03.023>

0012-821X/© 2015 Elsevier B.V. All rights reserved.

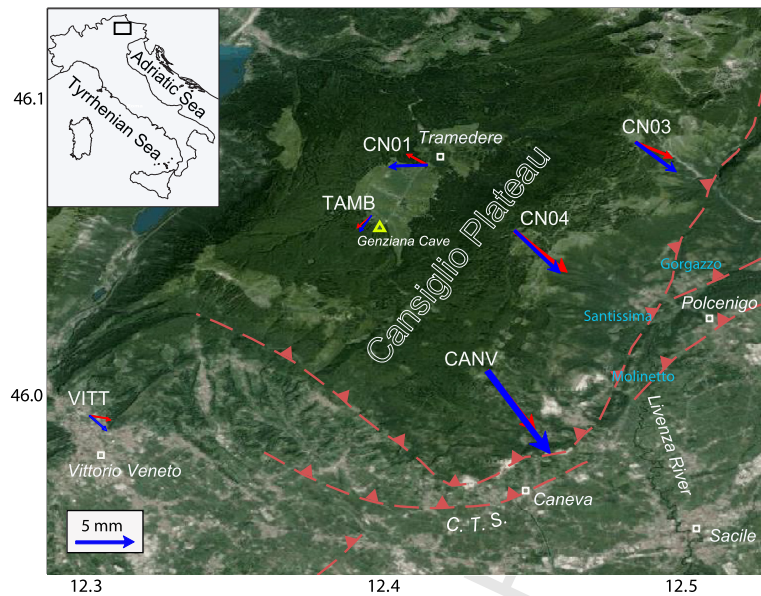


Fig. 1. Map of the Cansiglio Plateau area showing the Cansiglio Thrust System (C.T.S.) bordering the southeastern flanks of the Plateau. The four letter words represent the GPS station ID considered in this study, the red and blue arrows represent the displacements measured after two rain events in autumn 2011 (see text for more details). (For interpretation of the references to color in this figure, the reader is referred to the web version of this article.)

Evans and Wyatt, 1984; Kumpel et al., 1988; Takemoto, 1995; Dal Moro and Zadro, 1998; Braitenberg, 1999a; Jahr et al., 2008). More recently Longuevergne et al. (2009), Jacob et al. (2010) and Tenze et al. (2012) have successfully measured rock deformations induced by hydrological processes in different karst systems (respectively Vosges mountains, southern French Massif Central and classical Trieste karst). The first two investigations demonstrate that the observed karstic media deformations are likely due to water pressure changes in nearby fractures. Strain variations due to pumping experiments has been recently studied in California to constrain material properties of rock using the Darcy flow approximation (Barbour and Wyatt, 2014).

In this study, we test the hypothesis of hydrologic induced strain observed using both GPS and tiltmeter data in a karst system located in the southeastern Alps, the Cansiglio Plateau (CP), Italy (see Fig. 1 for location). Previous works in similar environments suggest that the occurrence of such phenomenon is not isolated and uncommon, but could be recurrent especially in karst areas providing new insights into hydrologic karst processes (Longuevergne et al., 2009; Jacob et al., 2010; Tenze et al., 2012; Diaz et al., 2014).

The CP is an extensive polje located in the southeastern Alps halfway between the Veneto and Friuli districts in Northeastern Italy. Its average height is about 1000 m above sea level (asl), bounded on the W–SE sides by a ridge of super elevated hills up to 1500 m asl. The whole CP is a limestone plateau with extensive karstic epigenetic and hypogenic features typical of a mature karst system, dolines are the most remarkable landscape features, both of dissolutional and collapse origin, and hundreds of caves have been identified, a few of them several hundred meters deep. The most sizable ones are: *Bus de la Genziana* 590 m depth, and *Abisso Col della Rizza*, reaching 800 m depth, both of them are regularly inspected by speleological expeditions. The southeastern slope of the CP is characterized by a thick succession of Cretaceous peritidal carbonates, while the central-western part is characterized by slope breccia deposits, all capped by basinal marly carbonates (Cancian et al., 1985). The surficial hydrography of CP is only modest and a deep aquifer, several hundreds of meters below the top of the CP, is supplied by infiltration of meteoric precipitation (up to 1800 mm/yr) through; dolines, sinkholes and conduits of prevalent vertical development. The aquifer yields significant quantities of

water to springs at the lower limb of the anticline, where the tectonized Mesozoic limestones are in contact with the Cenozoic and Quaternary impermeable units of the footwall. Three main springs at the foothills drain most of the CP water forming the Livenza River: Gorgazzo, Santissima and Molinetto, each bearing an average flow of 2–6 m³/s, yielding a total flow of about 11 m³/s (Vincenzi et al., 2011).

The Gorgazzo spring is a typical Vaclousian spring that originates from a shaft, a few meters of diameter, with the water running upwards. Occasionally, over periods of persisting drought, the piezometric surface is lowered below the outlet elevation and the spring dries up. Since no piezometric data are available, we presume that the springs at the foothills are located in a zone of intermittent saturation. A quantitative model of the hydrology of the CP has not been developed up to now and is therefore unavailable. In general, karst hydrology is complicated by the fact that the hydraulic conductivity is inhomogeneous and anisotropic due to the presence of fractures and shafts. Groundwater flows in the rock matrix, fractures and in conduits, where the conduit component (cave-like tubes) is significant.

Although matrix porosity has been shown to be important in providing storage capacity, the secondary porosity (conduits and fractures) dominates the pathways for groundwater flow (Ford and Williams, 2007, p. 104). In our case the rainfall response (input–output) relationships are the only means to treat the hydrologic system, as pumping experiments are not known to us. The latter are probably very difficult to accomplish, as the watertable is many hundreds meters below the surface. In the location of the tiltmeter the cave has been explored 600 m below surface before reaching the ground water level. Relying only on the rainfall response of the springs, the hydrologic system cannot be reliably parameterized. Parameters which could possibly be estimated and which contribute to drainage are gross specific yields and continuum transmissivity for the different portions of the aquifer (Shevenell, 2007). In order to accurately assess the deformation processes of karstified aquifers a detailed hydrologic study is necessary, due to the presence of well developed secondary porosity (fractures and fissures) and large conduits channeling most of the turbulent flow. Our study is focused on geodetic movements and inclinations of the CP karst plateau, and currently an accurate modeling of the

deformation cannot be fulfilled due to lack of constraining parameters on the hydraulic system.

The plateau is bounded on the southeast by a thrust fault (Caneva Thrust), part of the regional thrust system (Cansiglio Thrust System), that demonstrates Late Quaternary activity (Galadini et al., 2005). The main thrust plane is also associated with minor faults developing a quite wide cataclastic zone, about 500 m width. The most recent destructive earthquakes occurred in 1936 at the foot of the CP, associated to this thrust system with an $M = 5.8$ event at 15 km hypocentral depth (Sirovich and Pettenati, 2004).

At 33 km distance, in a very similar tectonic setting, the subsurface structures are being used for temporary storage of gas Methane (Edison, 2014), where periodically fluids are injected and extracted from the subsurface. Due to the analogous tectonic setting, the full understanding of the hydrologically induced deformations on the Cansiglio plateau could be useful to understand the role of water-induced deformations at the Methane deposit.

2. Data and method

Since 2005 the University of Trieste manages a tiltmeter station in a natural cave named “Bus de la Genziana” placed at 25 m depth (Grillo et al., 2011). This deep shaft has been recently demonstrated to be hydrologically connected to the drainage system of the Livenza River headwaters (Santissima and Molinetto) in the SE foothills of the Cansiglio (Vincenzi et al., 2011). The tiltmeters consist of two Marussi type, horizontal pendulums with Zöllner suspension oriented NS and EW. Each pendulum is hosted in a cast-iron conic housing and the records are digitalized with a nominal angular resolution of 2.5 nrad and a sampling rate of 1 h (Braitenberg, 1999b; Zadro and Braitenberg, 1999).

We also installed a few GPS stations and analyzed all available GPS data in order to characterize the regional surface deformation. Currently two permanent GPS stations on the CP are available: the Caneva station (CANV), part of the FReDNet geodynamic network (<http://www.crs.inogs.it/frednet>) owned by the OGS (Istituto Nazionale di Oceanografia e di Geofisica Sperimentale) and the Tambre station (TAMB) owned by the local governmental authority Regione Veneto (<http://147.162.229.63/Web>). The CANV station is materialized on a reinforced concrete pillar founded on the bedrock and the TAMB station is placed on the roof of a recently restored stone building. The GPS data were processed as described in Devoti et al. (2011), estimating daily station positions in the IGS08 reference system. We also filter out the common mode noise (Wdowinski et al., 1997) using 28 selected GPS stations positioned in a great circle of roughly 50 km radius around the CP, and compute the station residuals at CP stations subtracting the long term tectonic drift estimated at CANV station. The average root-mean-square (RMS) of the residuals of our station coordinates is 1.2 mm in the horizontal and 3.7 mm in the vertical components. CANV shows unusually high residuals in the horizontal plane, 3.3 mm in the north and 2.7 mm in the east component, which represents only about the fifth percentile of all the other station residuals.

The rainfall data were collected at the weather station located on the plateau, (loc. Tramedere, <http://www.arpa.veneto.it/>; see Fig. 1) placed at about 8 km north from CANV station and 2.5 km from the tiltmeter location, whereas the hydrometric station of the Livenza river is located at the foothills of the CP at about 4 km east from CANV station and 8 km east of the tiltmeter. The Livenza river is thought to be the main CP aquifer discharge but very few experimental data are currently available (see Vincenzi et al., 2011 for a discussion). We assume flow proportional to head, and thus water table variations proportional to streamflow variations. Since only the gauge height measurements are available continuously, we interpolate the streamflow measurements using a fourth or-

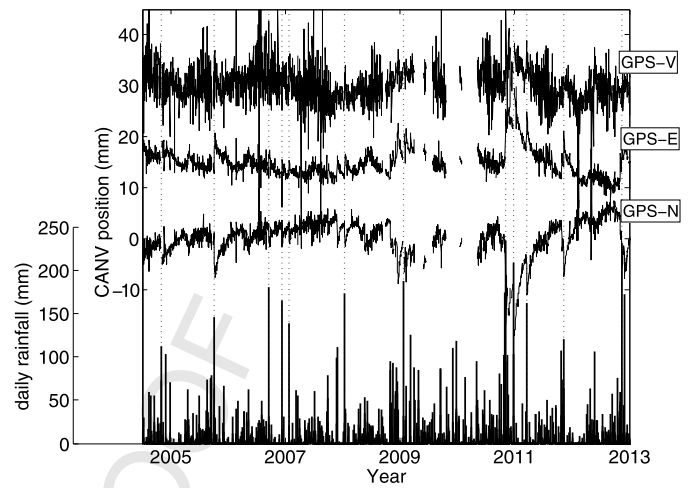


Fig. 2. Three dimensional position time series of the permanent GPS station (CANV) located on the Cansiglio Plateau (Italy), GPS-V, GPS-E and GPS-N are respectively the vertical, east and north components, the bar plot on the bottom represents the daily rainfall at Tramedere weather station. Major rain events are evidenced by vertical dashed lines.

der polynomial relationship (see auxiliary Fig. S1), and convert the hourly gauge heights to corresponding hourly streamflow values. We study the correlation of the tiltmeter and GPS anomalous displacements with the hydrologic parameters and discuss the results of an extensive GPS measurement campaign on the CP slopes that suggest the existence of a deformation anomaly acting at a regional scale (~ 10 km).

3. Results and modeling

From the beginning of its operation in 2004, the GPS permanent station CANV exhibits regular deformation patterns in the position time series, following each rain event. The daily positions show sudden displacements that, due to our temporal resolution, can be considered simultaneous to rain and are followed by a slow rebound towards the original position. Fig. 2 shows the GPS time series (GPS-E east, GPS-N north, GPS-V vertical) recorded at CANV station, together with the daily rainfall from the Tramedere weather station. The horizontal components (GPS-E and GPS-N) demonstrate remarkable shifts, roughly in the SSE direction, during rain episodes and the tendency to rebound in the following days or weeks resembling the time evolution of the Livenza gauge height. This is evidenced in Fig. 3 where the behavior of both GPS and tiltmeter measurements are compared during autumn and winter period 2010–2011. Three major rainfall events occur in that period: November, 2, December, 24 and March, 17 with respectively 502, 368 and 200 mm rainfall. In those days the GPS position shifts rapidly, respectively by 15, 13 and 10 mm in the SSE direction.

The long term behavior of the CANV time series seems to suggest a residual deformation originated from the karst-hydrological signal that cumulates over time. Fig. 4 displays the horizontal daily position residuals with respect to the secular drift of a nearby station (VITT, see Fig. 1 for the location), that well approximate the regional tectonic motion (~ 2 mm/yr towards N). For the sake of clarity the two time series are arbitrarily shifted by 10 mm, respectively upwards and downwards. The average long term drift in the E–W direction is similar in both stations, thus the residuals show no average drift, whereas in the N–S direction the CANV station appears delayed (residuals demonstrate a negative drift), especially noticeable after 2009 when the rainfall events are more frequent. We observe an average 1 mm/yr deficiency in the northern secular rate at CANV station, which can be interpreted as due to the anelastic part of the deformation that cumulates at each rainfall,

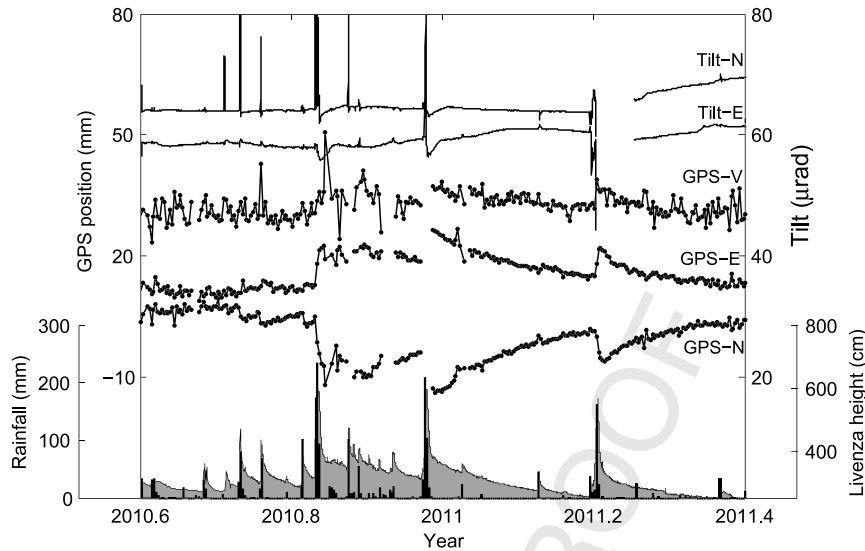


Fig. 3. Zoom of the daily GPS (GPS-V, GPS-E, GPS-N) and hourly tiltmeter (Tilt-N, Tilt-E) time series in the autumn–winter period 2010–2011. The tiltmeter observations are smoothed out with a running box window of 6 h. The daily rainfall (bars) and Livenza river gauge height (gray filled area) is also reported in the bottom of the graph.

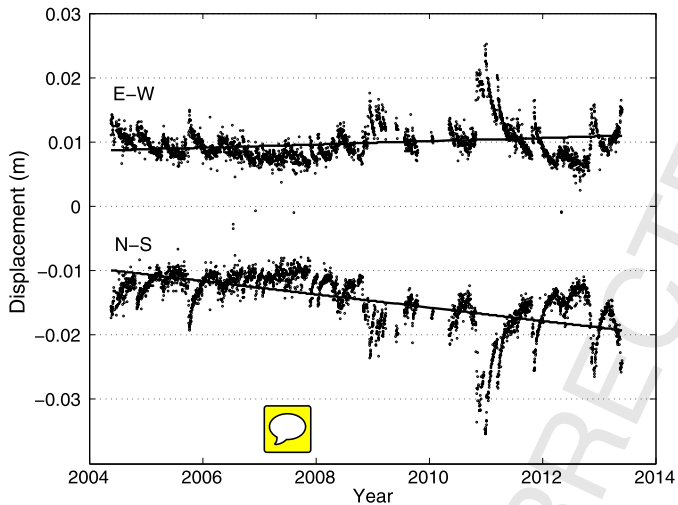


Fig. 4. Different secular rates measured at CANV and VITT permanent stations. Dots represent the CANV daily position in the horizontal directions, North–South (N–S) and East–West (E–W). Straight lines represent the secular rates of CANV (solid line) and VITT (dashed line). VITT is a nearby permanent GPS station assumed to properly measure the regional tectonic drift.

or alternatively caused by the incomplete elastic rebound during specific heavy rainy periods marked by an incomplete aquifer discharge.

During the operational period of the CANV station (2004.5–2013.4) we identified a total of 57 rain episodes characterized by uninterrupted rain, each of them lasting between 13 and 116 h. In this period we observe an average annual rainfall of 920 mm, with events ranging from a minimum of 47 mm to a maximum of 502 mm. We estimate the corresponding 3-D GPS displacements computing the difference between post- and pre-event average station position. Furthermore at the same epochs we were able to measure the gauge height variations of the discharge river. The correlations of GPS displacements with rainfall and with gauge heights (or alternatively with the river streamflow) are high for the horizontal displacements and insignificant for the vertical displacement. The significance of the correlation coefficient is estimated using a Student's *t*-test to test the null hypothesis of zero correlation. We define the critical correlation as being the value of correlation, above which the *t*-test rejects the null hypothesis at the 95%

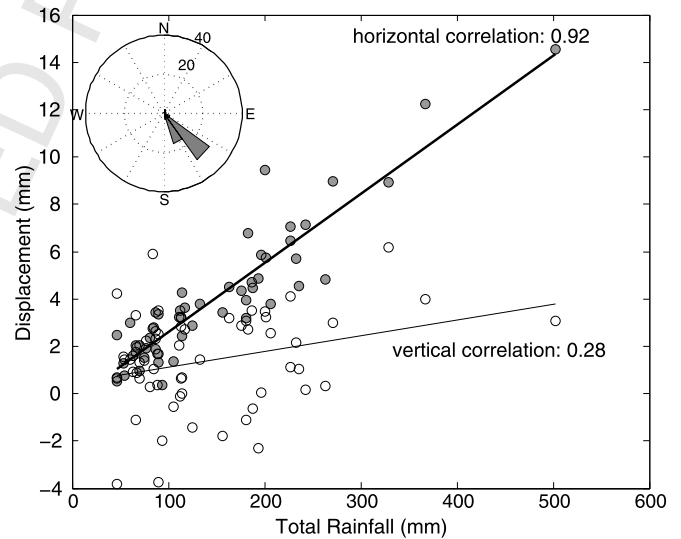


Fig. 5. Displacements versus rainfall amount as observed at CANV GPS station. The grey circles represent the horizontal displacements whereas the open circles, the vertical displacements. The inset shows the polar histogram of the displacement directions of all (57) rain events.

confidence level, in other words it represents the minimum correlation coefficient below which the variables can be considered uncorrelated. At this confidence level the vertical GPS displacements could be considered uncorrelated with rain (0.28) and with other hydrologic quantities, being always below the critical correlation coefficient (0.3). The horizontal displacements are instead significantly correlated with rainfall (0.92), with the gauge height variations (0.71) and streamflow variations (0.63). Fig. 5 shows the correlation plot for the GPS horizontal and vertical displacements versus rainfall. The horizontal displacement is remarkably proportional to the amount of rainfall (2.9 mm every 100 mm of accumulated rainfall). We note that the deformation is correlated to a lesser extent with the river gauge height variations (or discharge streamflow) and hence with water table variations. This is a strong indication that the cause of the deformation is more directly linked with subsurface hydrologic processes in the karstic vadose zone rather than with deep rooted water table variations in the phreatic zone. This observation is in agreement with the

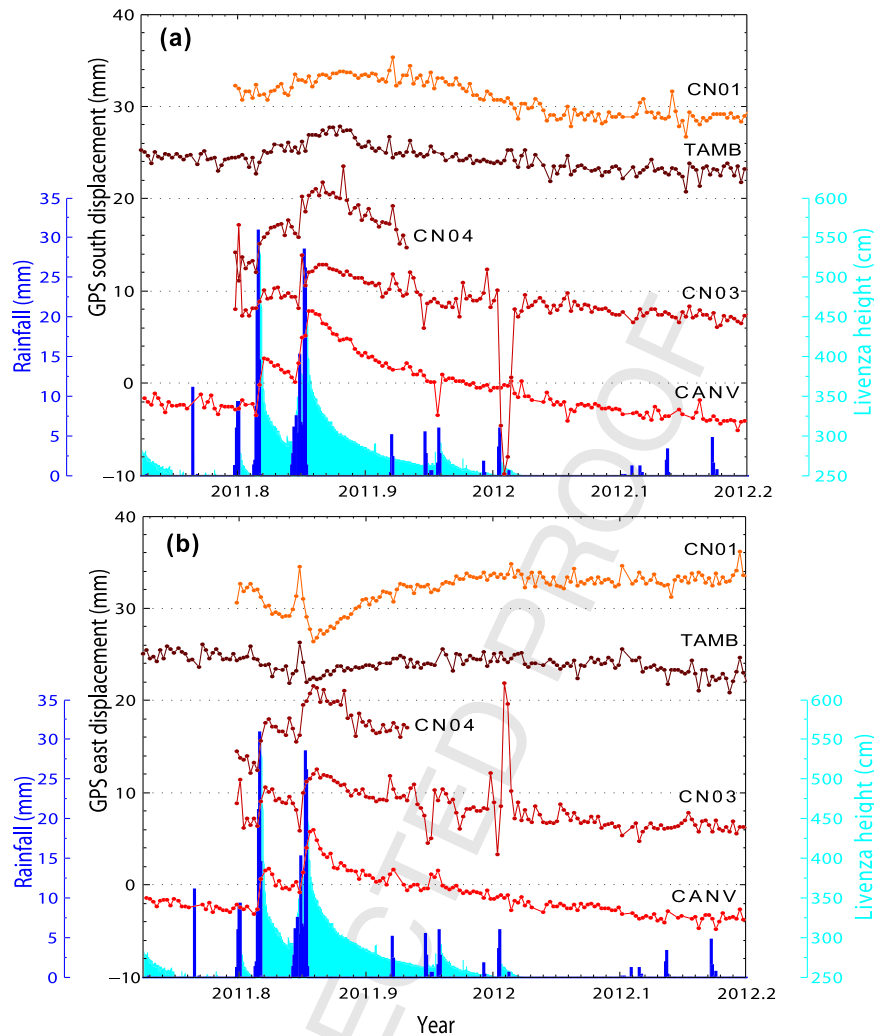


Fig. 6. GPS time series of the intensive measuring campaign during winter 2011–2012. Panel a) shows the daily station positions in the south direction and panel b) shows the station positions in the east direction. The rainfall (blue bars) and Livenza river gauge height (cyan filled area) is reported in the bottom of the graphs. (For interpretation of the references to color in this figure legend, the reader is referred to the web version of this article.)

main findings of Longuevergne et al. (2009) and Jacob et al. (2010) that identify hydrologically active fractures in the vadose zone as sources of their observed tilt variations.

In order to ascertain the spatial limits of the deformation pattern, we installed five GPS stations on the top of the CP and carried out an intensive measurement campaign during winter 2011–2012. The GPS antennas were mounted on geodetic benchmarks, anchored on outcrops of the plateau. Each benchmark, made by a stainless steel rod, has been drilled in the bedrock at a variable depth of 0.5–0.8 m and fastened with epoxy resins. During the measurement campaign two significant rain events occurred (on October, 26 and November 8 with respectively 183 and 271 mm rainfall), causing recognizable surface displacements at other three stations. Fig. 1 shows the displacement vectors recorded at all available stations for the two rain events, indicated respectively with the red and blue arrows. The horizontal GPS time series are shown in Fig. 6, three stations (CN03, CN04 and CANV) demonstrate abrupt variations in correspondence of the rain events, followed by a slow rebound that fully recovers the original pre-event position. Other two stations located on the plateau (TAMB and CN01) show minor, or no reaction to the rain. The vertical time series are shown in the auxiliary Fig. S2 and are less affected by rainfall occurrences (e.g. CANV, CN03 and CN01), and show different responses to rain. The GPS campaign evidences the scale of the phenomenon, at least $12 \times 5 \text{ km}^2$ area is subject to a coherent de-

formation, involving the whole southeastern slope of the CP that reacts to hydrological stresses. The stations bordering the southeastern slope are displaced by an amount of 4–9 mm by heavy rain, whereas the plateau is rather motionless or moving in the opposite direction. Very interesting are the anomalous displacements visible at the station CN03 in the first few days of year 2012. The GPS station, in spite of being anchored on outcrop, shows a sudden back and forth displacement spanning a few centimeters and lasting only 4–5 days, it seems a very local effect (confined only at CN03) and apparently not permanent (it doesn't show hysteresis), the cause of these oscillations has not yet been identified and is still under investigation.

The tiltmeter time series demonstrate a clear causal relationship with the pluviometric and the hydrometric data, but its variations are not as regular as the GPS. The tilt variations in correspondence of rainfall vary from fractions of micro-radians, up to 30 μrad and exhibit sudden spikes in both the N–S and E–W directions, generally more pronounced in the N–S direction (see Figs. 3 and 7). These variations are two orders of magnitude larger than solid Earth tides tilt variations. The observed impulsive tilts show sporadic changes in the direction, tilt variations are mostly directed towards N or NNW (75%) but sometimes, and to a less extent, flip to the opposite direction (25%) (Grillo et al., 2011). In order to assess the tiltmeter response, we further zoom into the event of December 2010 (Fig. 7), where the displayed recordings

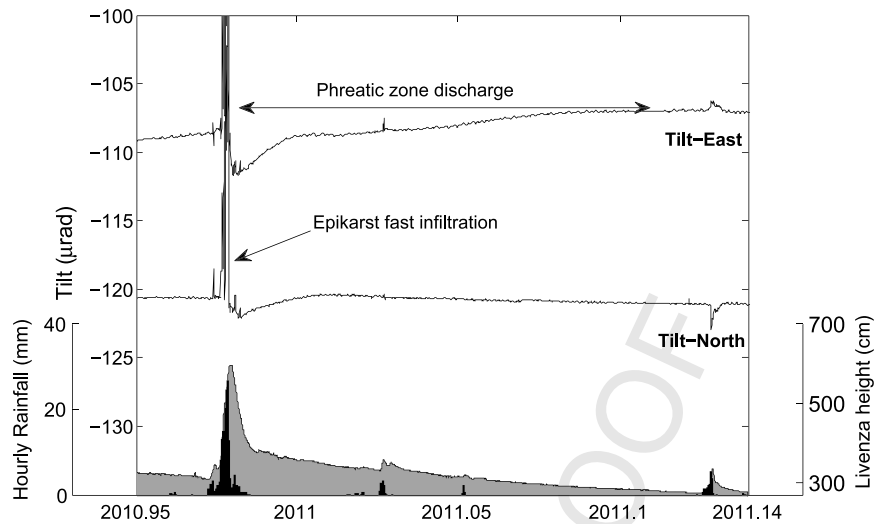


Fig. 7. Zoom on tiltmeter evolution (East and North components) on December 2010. Rainfall (black bars), tilt data (solid lines) and gauge heights (gray filled area) are all sampled at hourly intervals.

of tilt and rain are sampled at hourly intervals. The tilt response to rainfall is first a back-and-forth movement towards N-NE, almost contemporaneous to rain and lasting only a few hours, followed by a successive slow rebound over days that is similar to the GPS and the Livenza gauge height trends. To characterize the fast-moving tilt spikes we automatically detect the transients of tilt amplitudes (EW-NS modules) after eliminating the long-period trend from the data (low pass filter with cut off at 1/70 days, cosine filter tapering). A tilt spike is identified if its variation is greater than 1.5 times the noise-threshold, the latter defined as the double standard deviation of the detrended data. At each spike epoch we determine the duration of the anomalous variation. Fig. S3 shows the histogram of time lags for the 57 detected spike events, it evidences the very fast response to rainfall lasting only a few hours with long lasting tilts up to 11 h for the more intense rainfalls. To evaluate the tilt-rainfall correlation, we integrate the rain in a time window right before the spike epoch, choosing the window span being equal to the spike duration and placing the tail of the window at the spike epoch. Fig. S4 shows the scatterplot and the linear interpolation of tilt and rainwater, we obtain a correlation coefficient of 0.38 which results to be just above the critical threshold. In conclusion the spikes are very short lived events, which correspond to the fast runoff of rainwater through the highly fractured epikarst. This fast infiltration is obviously below the resolution capability of our GPS time series. The prevalent NNW tilting direction is however coherent with the observed GPS displacement direction.

The discharge style of the karst aquifer can be tracked down from the stream hydrographs of the Livenza river. The maximum flow is systematically delayed with respect to the rain peaks by a time lag that depends on the groundwater travel path through the karst system. The time lag represents the travel time the rainwater needs to reach the bottom of the hill. Analyzing the entire dataset we estimated a time lag of 9 h (median), which reflects the characteristic conductivity of the entire karst system for the rapid flow through the most receptive conduits. In Fig. 8 we plot the streamflow trends of the recession phase after main floods in a semi-logarithmic scale. Linear trends in the logarithmic hydrographs follow from a linear relation between hydraulic head and flow rate, which is commonly found in karst baseflow (Maillet, 2003). Almost all recession curves in Fig. 8 are characterized by a rapid runoff phase lasting 10–48 h, followed by a slow discharge rate lasting a few weeks (dashed lines show the prevailing trends). We evaluate the following half periods (i.e. the time required for

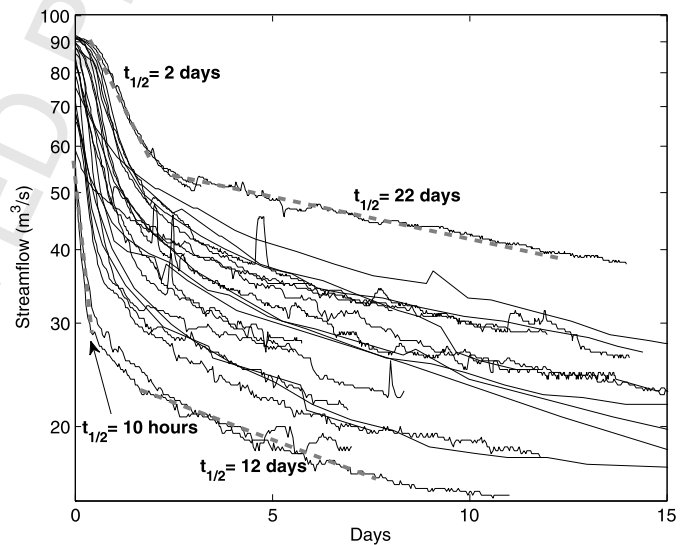


Fig. 8. Livenza stream hydrographs of the recession curves after floods. The dashed lines represent the average trends of the recession curves of the river in the fast flow (10–48 h) and slow flow (12–22 days) phases.

the streamflow to halve) for the fast discharge ($t_{1/2} = 10$ h to 2.3 days) and for the slow discharge ($t_{1/2} = 12$ to 22 days). Therefore the initial rapid flow in shafts and conduits through the vadose zone, causes the baseflow to rise to its maximum within 9 h after the rainfall peak, and it persists in proportion to the total rainfall corresponding to the observed rapid runoff (10–48 h). In this stage the effective hydraulic conductivity of the whole karst system is of the order of $4\text{--}5 \cdot 10^{-2}$ m/s, which is characteristic of flows through coarse gravels. This phase ends within the first 48 h after the flood and saturates eventually the secondary porosity (fractures and fissures) of the rock matrix. Afterwards the drainage progresses slowly, fed mainly by infiltration through the secondary porosity of the karstic medium, similarly to what has been observed in different contexts (e.g. Shevenell, 2007). In this stage the conductivity reduces by two orders of magnitude to about $7 \cdot 10^{-4}$ m/s (assuming 17 days of average decay time), corresponding to an intrinsic permeability of 10^{-10} m², which is still several orders of magnitude higher than the permeability observed in unfractured porous limestones (e.g. Jaeger et al., 2003). Thus we infer that the slower drainage is caused mainly by the secondary

porosity as a response from narrower fissures and fractures. Assuming a Darcian flow and assuming the validity of the cubic law for the flow through fissures (Witherspoon et al., 1980), we evaluate an equivalent fracture opening of 40–50 μm to explain the observed flow. Thus we conclude that the drainage through a connected texture of fractures and fissures is not negligible and may well explain the observed permeability.

The change in strain induced by a sub-vertical fracture may be properly modeled in the far-field by a simple Okada-type model (Okada, 1985). A single vertical tensile source is used to model the expected deformation in a homogeneous elastic medium. This idealized source could be a very crude approximation of the complex karstic fractures system, in which the observed displacements result from the cumulating effect of distinct individual sources. However the simplified model is useful for arguing on properties of the source geometry, even though only achieving qualitative findings. Fig. S5, panel a), shows the expected displacement field of a vertically oriented rectangular source, simulating a tensile dislocation of 2 cm, in a typical elastic medium (modulus of rigidity $G = 30$ GPa and Poisson ratio $\nu = 0.25$) computed using dMODELS software (Battaglia et al., 2013). Panel b of Fig. S5 shows the profile of the predicted surface displacement and tilt across the source strike. It is worthwhile to note that the displacement and angular observables decay at different rates at increasing distance from the source. Strong tilt variations, up to tens of μrad , will occur only in the near proximity of the source (within 5% of the total source length), whereas the surface displacements demonstrate a longer wavelength, being greater than millimeters at substantial proportions of the source length (within 80% of the total length). Therefore, given the observed displacements and tilt variations on the CP, we expect the tiltmeter being particularly sensitive to nearby fractures whereas, on the contrary, the GPS being sensitive to a wider integrated source domain. Another important conclusion arises from the ratio between the horizontal and vertical displacement (h/v) observed at the CANV station. We derive the h/v proportion computing the ratio between the average horizontal and vertical deformations (straight lines in Fig. 5), estimating a mean value of $h/v = 2.5$. This value can be considered as a ceiling threshold for the h/v ratio since, on the average, no higher values are expected at CANV station. In Fig. 9 we simulate a family of maximum h/v values achieved with variable source width and tip depth. At $h/v = 2.5$, and increasing the source width, the curves show a corresponding increase in the tip depth of the source, so that width and depth are the same. Thus the curves suggest that the source width should be at least as wide as the tip depth, such that a near surface fracture is in proportion shorter (small source width) than a deeper one and conversely, long fracture paths should extend very deep in the mountain. Since these conclusions rely on a single GPS observing station we cannot draw any definitive conclusion until more monitoring stations are available in order to figure out a more realistic source geometry.

The observed high tilt variations (on the order of μrad) could only be obtained with shallow sources, and also the change in direction of the tilt, peculiar of the CP (this publication and Grillo et al., 2011 compared to e.g., Braitenberg, 1999b; Tenze et al., 2012), demand for a complex system of nearby fractures placed at different depths and relative positions. The change in direction of the tilt is peculiar of the Cansiglio Plateau, as it has not been observed in the other tiltmeter stations of the same network. As an example, we could imagine that the geodetic stations first sense an upper crack and move in one direction, then a lower crack is filled, and the induced signal is summed to the first one, creating the direction inversion in the tilt response and possibly also in the GPS measurement, depending on the relative positions.

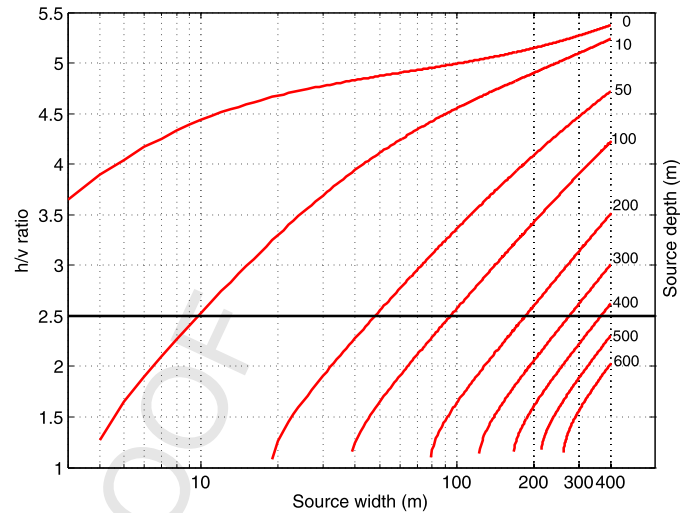


Fig. 9. Modeled deformation ratio (h/v) for a family of vertical tensile sources varying in tip depth (shown on the right) plotted against the source width. At CANV station we observe a characteristic ratio of $h/v = 2.5$ (highlighted).

4. Discussion and conclusion

The GPS displacements of the stations located at the flanks of the CP show statistically significant correlations with the karst hydrologic system, showing a very fast and impulsive response to rainfall. We find that the permanent GPS station at Caneva (CANV), with 8 yr of continuous recordings, shows a succession of displacements triggered by moderate to heavy rainfall, showing a repetitive time evolution. The cross-correlation analysis between the observed GPS horizontal deformation and of the hydrological quantities, all demonstrate significant positive correlation. The strongest correlation being with the local rainfall, evidencing that surficial hydrologic processes are the most probable cause of the observed deformation. A couple of tiltmeters, installed in a cave at the top of the plateau, show a less regular reaction to rainfall compared to the GPS stations. The two hydrologically induced signals are distinct in their temporal evolution, which is due to the different settings of the stations (flanks or top of plateau) and to different sensitivities to ongoing processes. The geodetic measurements, as also the streamflow data show time constants of several days, as they collect the water of the entire plateau. During the rain episodes the tilt response is much more rapid and wide (in the order of hours and up to tens of μrad). For a subset of rain events, three temporary GPS stations located in different places on the flanks of the Plateau, confirm the transient deformation demonstrating an outboard oriented pattern of the deformation in response to rain. After rainfall exceeding 40 mm, the whole plateau expands laterally in all directions, with only small vertical deformation. The hydrologic induced movement observed at GPS stations, is distinctive for the Cansiglio area, such strong effects have not yet been observed in other GPS stations of the southeastern Alps.

The water intake of rainfall is drained through fissures and fractures of the carbonate platform of the CP and emerges at the foot of the plateau from a Vauculian-type spring, forming the Livenza River. The river responds to rainfall episodes by a rapid increase of the hydrometric height (maximum height reached 9 h after the rainfall centroid) and followed by at least two distinct runoff phases: a rapid discharge phase (runoff) lasting 10–48 h and a slow discharge phase (infiltration) lasting a couple of weeks. We argue that the fast runoff phase, characterized by a high hydraulic conductivity, represents the early rainwater flow through open sinkholes and conduits reflecting a turbulent flow through

the karst. In parallel the drainage progresses as infiltration through fractures and fissures, flowing with a slower discharge rate. In this latter phase the permeability reduces by two orders of magnitude, which is still several orders of magnitude higher than the permeability of unfractured limestones. We speculate that a congruous contribution to the drainage may derive from a connected texture of fractures of 40–50 μm effective aperture width, most probably of tectonic origin, i.e. shallow normal faults or extrados fractures formed on the anticlinal crest (Philip and Meghraoui, 1983; Galadini et al., 2001). The lineament analysis of the CP based on Landsat ETM+ imagery (Vincenzi et al., 2011), identifies two main patterns along the NW–SE and NNE–SSW directions which are respectively parallel and orthogonal to the observed GPS horizontal displacement (see Fig. 5 for GPS directivity). These lineaments follow the basic active tectonic structures bordering the CP and are the most probable sources for promoting large scale deformations caused by active fractures along the CP slopes. We suggest that micron-sized fractures, filled by rainwater cause a prompt strain release, followed by a slow rebound as groundwater discharges through fractures. Current data and observations on the CP do not allow a reliable estimate of any source parameter, but a simple elastic model suggests that active sources should be as deep as its length (source width). Since every 100 m of water column exerts a stress of 1 MPa, any deep-rooted fracture, tending to seal with depth, may well explain the observed surface lateral deformation observed at the flanks of the plateau.

Concerning the tiltmeters, albeit the hydrologic induced tilt is generally observed, its impulsive nature is atypical in this location. The typical signal of the other stations in the southeastern Alps is limited to a response of smaller amplitude and lasting several days. The underground tiltmeter and the GPS are observing different phenomena related to the hydrologic system. The tiltmeter is susceptible to the small scale infiltration into the network of fissures of the most shallow layer of the karst in the epikarst. This is the superficial fractured layer of the karst plateau, which can be up to 20 m thick, overlying the more compact limestones. The water flows in the epikarst at much higher velocity than the water drainage in the underlying layer due to the high volume percentage of fractures, generally over 20% (Ford and Williams, 2007, p. 133). At the tiltmeter location, the quantity of rainwater is only a fraction of the total flux supplying the springs at the base of the plateau. The amount of the observed tilt deformation is orders of magnitude smaller than the movements observed for instance by the GPS permanent station TAMB (installed at 400 m from the tiltmeter). For instance a tilting of 1 μrad of a structure in the epikarst layer (characteristic length of 10 m), would produce a horizontal movement of only 10^{-5} m, too small to be detected by the GPS, but well in the measuring range of the tiltmeter. Due to the small hydrologic volumes involved, the deformation at the epikarst is therefore only seen by the tiltmeters. Due to the complicated network of hydraulic conduits in the epikarst, the tilt signal can change in direction, though maintaining a preferred tilt direction. Due to the higher hydraulic conductivity of the epikarst respect to the underlying more compact layer, the water forms a temporary aquifer at the bottom of the epikarst. We suspect that the complicated tilt response is due to the formation of this temporary aquifer, which only forms if a threshold value of precipitation has been passed.

The present study demonstrates the direct link between the aquifer system cycles and the induced surface deformation, providing interesting insights of karst style hydrological processes, that could also be relevant in the assessment of hydrologic hazards. The GPS and the tilt observations are complementary and sensitive enough to study and monitor the effects of water infiltration in karst systems. The question arises whether a near real-time monitoring of the hydrologic deformation can provide useful in-

formation to assess or predict seasonal hydrologic cycles and associated environmental hazards in specific conditions, e.g. triggering of landslides and rock avalanches, well recognized on both SW and SE slopes by the Livenza Basin Authority (<http://www.adbve.it>).

Acknowledgements

We would like to offer our special thanks to Sergio Del Mese, who helped us in conducting the GPS measurement campaigns. We are also particularly grateful for the assistance given by Adriano Cavaliere in the construction of the geodetic benchmarks. Advice given by Alessandra Esposito, Emanuela Falcucci and Stefano Gori and their fruitful discussions with RD on many subjects of this work have been a great help in improving the manuscript. Dr. Ildiko' Nagy is thanked for maintaining the tilt database. Assistance given by rangers of the Corpo Forestale dello Stato, stazione Pian del Consiglio and Vittorio Veneto was greatly appreciated. The GPS data are available at <http://www.crs.inogs.it/frednet> or may be requested to the first author. We would like to thank the regional administration authority "Regione Veneto", the OGS (Istituto Nazionale di Oceanografia e di Geofisica Sperimentale) and the University of Padova, that make the GPS data available to the public domain. We thank ARPA-Veneto Teolo Meteorologic Center for the concession of rainfall data, Ivan Di Fant and Ing. Giorgio Dalla Chiesa (Central Environmental Management and Public Works – Hydrographic Unit – Friuli Venezia Giulia Region) for the Livenza hydrometric data. Finally we thank two anonymous reviewers for their constructive comments that enhanced the analysis of the hydrologic data.

Appendix A. Supplementary material

Supplementary material related to this article can be found online at <http://dx.doi.org/10.1016/j.epsl.2015.03.023>.

Uncited references

(Milanović, 1976) (Meneghel et al., 1986)

References

- Argus, D.F., Heflin, M.B., Peltzer, G., Crampé, F., Webb, F.H., 2005. Interseismic strain accumulation and anthropogenic motion in metropolitan Los Angeles. *J. Geophys. Res.* 110, B04401. <http://dx.doi.org/10.1029/2003JB002934>.
- Barbour, A.J., Wyatt, F.K., 2014. Modeling strain and pore pressure associated with fluid extraction: the Pathfinder Ranch experiment. *J. Geophys. Res., Solid Earth* 119, 5254–5273. <http://dx.doi.org/10.1002/2014JB011169>.
- Battaglia, M., Cervelli, P.F., Murray, J.R., 2013. dMODELS: a MATLAB software package for modeling crustal deformation near active faults and volcanic centers. *J. Volcanol. Geotherm. Res.* 254, 1–4.
- Bawden, G.W., Thatcher, W., Stein, R.S., Hudnut, D.W., Peltzer, G., 2001. Tectonic contraction across Los Angeles after removal of groundwater pumping effects. *Nature* 412, 812–815. <http://dx.doi.org/10.1038/35090558>.
- Braitenberg, C., 1999a. Estimating the hydrologic induced signal in geodetic measurements with predictive filtering methods. *Geophys. Res. Lett.* 26, 775–778.
- Braitenberg, C., 1999b. The Friuli (NE Italy) tilt/strain gauges and short term observations. *Ann. Geofis.* 42, 1–28.
- Braitenberg, C., 2000. Non-random spectral components in the seismicity of NE Italy. *Earth Planet. Sci. Lett.* 179 (2), 379–390.
- Caloi, P., Migani, M., 1972. Movements of the fault of the Lake of Cavazzo in connection with the local rainfalls. *Ann. Geophys.* 25 (1), 15–20. <http://dx.doi.org/10.4401/ag-5098>.
- Cancian, G., Ghetti, S., Semenza, E., 1985. Aspetti geologici dell'altopiano del Cansiglio. In: *Lav. - Soc. Ven. Sci. Nat.*, vol. 10 (suppl.), Venezia 1985, pp. 79–90.
- Dal Moro, G., Zadro, M., 1998. Subsurface deformations induced by rainfall and atmospheric pressure: tilt/strain measurements in the NE-Italy seismic area. *Earth Planet. Sci. Lett.* 164 (1–2), 193–203. [http://dx.doi.org/10.1016/S0012-821X\(98\)00203-9](http://dx.doi.org/10.1016/S0012-821X(98)00203-9).
- Devoti, R., Esposito, A., Pietrantonio, G., Pisani, A.R., Riguzzi, F., 2011. Evidence of large scale deformation patterns from GPS data in the Italian subduction boundary. *Earth Planet. Sci. Lett.* 311, 230–241. <http://dx.doi.org/10.1016/j.epsl.2011.09.034>.

- 1 Diaz, J., Ruiz, M., Crescentini, L., Amoroso, A., Gallart, J., 2014. Seismic monitoring
2 of an Alpine mountain river. *J. Geophys. Res.* 119, 3276–3289. [http://dx.doi.org/](http://dx.doi.org/10.1002/2014JB010955)
3 [10.1002/2014JB010955](http://dx.doi.org/10.1002/2014JB010955).
- 4 Edge, R.J., Baker, T.F., Jeffries, G., 1981. Borehole tilt measurements: aperiodic crustal
5 tilt in an aseismic area. *Tectonophysics* 71, 97–109. [http://dx.doi.org/10.1016/](http://dx.doi.org/10.1016/0040-1951(81)90052-4)
6 [0040-1951\(81\)90052-4](http://dx.doi.org/10.1016/0040-1951(81)90052-4).
- 7 Edison, 2014. Edison Stocaggio Spa, Centrale Stocaggio Gas, Campo Collalto.
8 <http://www.edisonstocaggio.it/stocaggio/content/campo-collalto> (last visited
9 29/07/2014).
- 10 Evans, K., Wyatt, F., 1984. Water table effects on the measurement of Earth strain.
11 *Tectonophysics* 108, 323–337. [http://dx.doi.org/10.1016/0040-1951\(84\)90242-7](http://dx.doi.org/10.1016/0040-1951(84)90242-7).
- 12 Ford, D., Williams, P., 2007. *Karst Hydrogeology and Geomorphology*. Wiley,
13 ISBN 978-0-470-84996-5, pp. 1–578.
- 14 Galadini, F., Galli, P., Cittadini, A., Giaccio, B., 2001. Late quaternary fault movements
15 in the Mt. Baldo–Lessini Mts. sector of the Southalpine area (northern Italy).
16 *Neth. J. Geosci.* 80 (3–4), 187–208.
- 17 Galadini, F., Poli, M.E., Zanferrari, A., 2005. Seismogenic sources potentially re-
18 sponsible for earthquakes with $M > 6$ in the eastern Southern Alps (Thiene–
19 Udine sector, NE Italy). *Geophys. J. Int.* 161, 739–762. [http://dx.doi.org/10.1111/](http://dx.doi.org/10.1111/j.1365-246X.2005.02571.x)
20 [j.1365-246X.2005.02571.x](http://dx.doi.org/10.1111/j.1365-246X.2005.02571.x).
- 21 Grillo, B., Braitenberg, C., Devoti, R., Nagy, I., 2011. The study of Karstic aquifers
22 by geodetic measurements in Bus de la Genziana station – Cansiglio Plateau
23 (Northeastern Italy). *Acta Carsol.* 40 (1), 161–173.
- 24 King, N.E., et al., 2007. Space geodetic observation of expansion of the San Gabriel
25 Valley, California, aquifer system, during heavy rainfall in winter 2004–2005.
26 *J. Geophys. Res.* 112, B03409. <http://dx.doi.org/10.1029/2006JB004448>.
- 27 Kumpel, H.-J., Peters, J.A., Bower, D.R., 1988. Nontidal tilt and water table variations
28 in a seismically active region in Quebec, Canada. *Tectonophysics* 152, 253–265.
29 [http://dx.doi.org/10.1016/0040-1951\(88\)90051-0](http://dx.doi.org/10.1016/0040-1951(88)90051-0).
- 30 Jacob, T., Chéry, J., Boudin, F., Bayer, R., 2010. Monitoring deformation from hydro-
31 logic processes in a karst aquifer using long-baseline tiltmeters. *Water Resour.*
32 *Res.* 46, W09542. <http://dx.doi.org/10.1029/2009WR008082>.
- 33 Jahr, T., Jentzsch, G., Gebauer, A., Lau, T., 2008. Deformation, seismicity, and flu-
34 ids: results of the 2004/2005 water injection experiment at the KTB/Germany.
35 *J. Geophys. Res.* 113, B11410. <http://dx.doi.org/10.1029/2008JB005610>.
- 36 Ji, K.H., Herring, T.A., 2012. Correlation between changes in groundwater levels and
37 surface deformation from GPS measurements in the San Gabriel Valley, Califor-
38 nia. *Geophys. Res. Lett.* 39, L01301. <http://dx.doi.org/10.1029/2011GL050195>.
- 39 Lanari, R., Lundgren, P., Manzo, M., Casu, F., 2004. Satellite radar interferometry time
40 series analysis of surface deformation for Los Angeles, California. *Geophys. Res.*
41 *Let.* 31, L23613. <http://dx.doi.org/10.1029/2004GL021294>.
- 42 Longuevergne, L., Florsch, N., Boudin, F., Oudin, L., Camerlynck, C., 2009. Tilt
43 and strain deformation induced by hydrologically active natural fractures:
44 application to the tiltmeters installed in Sainte-Croix-aux-Mines observatory
45 (France). *Geophys. J. Int.* 178, 667–677. [http://dx.doi.org/10.1111/j.1365-246X.](http://dx.doi.org/10.1111/j.1365-246X.2009.04197.x)
46 [2009.04197.x](http://dx.doi.org/10.1111/j.1365-246X.2009.04197.x).
- 47 Milanović, P., 1976. Water regime in deep karst. Case study of the Ombla spring
48 drainage area. In: Yevjevich, V. (Ed.), *Karst Hydrology and Water Resources*. In:
49 *Karst Hydrology*, vol. 1. Water Resources Publications, Colorado, pp. 165–191.
- 50 Meneghel, M., Sauro, U., Baciga, M.L., Fileccia, A., Frigo, G., Toniello, V., Zampieri, D.,
51 1986. Sorgenti carsiche e erosione chimica nelle Prealpi Venete (Karstic springs
52 and chemical erosion in the area of Prealpi Venete). *Studi Trent. Sci. Nat., Acta*
53 *Geol.* 62, 145–172.
- 54 Okada, Y., 1985. Surface deformation due to shear and tensile faults in a half-space.
55 *Bull. Seismol. Soc. Am.* 75 (4), 1135–1154.
- 56 Philip, H., Meghraoui, M., 1983. Structural analysis and interpretation of the sur-
57 face deformations of the El Asnam Earthquake of October 10, 1980. *Tectonics* 2,
58 17–49. <http://dx.doi.org/10.1029/TC002i001p00017>.
- 59 Shevenell, L., 2007. Analysis of well hydrographs in a karst aquifer: estimates of
60 specific yields and continuum transmissivities. *J. Hydrol.* 174, 331–355.
- 61 Sirovich, L., Pettenati, F., 2004. Source inversion of intensity patterns of earthquakes:
62 a destructive shock in 1936 in northeast Italy. *J. Geophys. Res.* 109, B10309.
63 <http://dx.doi.org/10.1029/2003JB002919>.
- 64 Takemoto, S., 1995. Recent results obtained from continuous monitoring of crustal
65 deformation. *J. Phys. Earth* 43, 407–420. [http://dx.doi.org/10.4294/jpe.1952.](http://dx.doi.org/10.4294/jpe.1952.43.407)
66 [43.407](http://dx.doi.org/10.4294/jpe.1952.43.407).
- 67 Tenze, D., Braitenberg, C., Nagy, I., 2012. Karst deformations due to environmental
68 factors: evidences from the horizontal pendulums of Grotta Gigante, Italy. *Boll.*
69 *Geofis. Teor. Appl.* 53, 331–345. <http://dx.doi.org/10.4430/bgta0049>.
- 70 Vincenzi, V., Riva, A., Rossetti, S., 2011. Towards a better knowledge of Cansiglio
71 karst system (Italy): results of the first successful groundwater tracer test. *Acta*
72 *Carsologica* 40 (1), 147–159.
- 73 Wdowinski, S., Bock, Y., Zhang, J., Fang, P., Genrich, J., 1997. Southern California
74 Permanent GPS Geodetic Array: spatial filtering of daily positions for estimat-
75 ing coseismic and postseismic displacements induced by the 1992 Landers
76 earthquake. *J. Geophys. Res.* 102 (B8), 18057–18070. [http://dx.doi.org/10.1029/](http://dx.doi.org/10.1029/97JB01378)
77 [97JB01378](http://dx.doi.org/10.1029/97JB01378).
- 78 Witherspoon, P.A., Wang, J.S.Y., Iwai, K., Gale, J.E., 1980. Validity of cubic law for
79 fluid flow in a deformable rock fracture. *Water Resour. Res.* 16 (6), 1016–1024.
- 80 Zadro, M., Braitenberg, C., 1999. Measurements and interpretations of tilt-strain
81 gauges in seismically active areas. *Earth-Sci. Rev.* 47, 151–187. [http://dx.doi.org/](http://dx.doi.org/10.1016/S0012-8252(99)00028-8)
82 [10.1016/S0012-8252\(99\)00028-8](http://dx.doi.org/10.1016/S0012-8252(99)00028-8).



ELSEVIER

Contents lists available at ScienceDirect

Earth and Planetary Science Letters

www.elsevier.com/locate/epsl



Graphical abstract

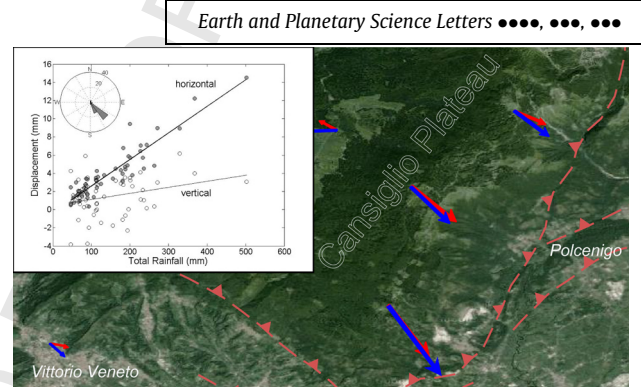
Hydrologically induced slope deformations detected by GPS and clinometric surveys in the Cansiglio Plateau, southern Alps

R. Devoti^{a,*}, D. Zuliani^b, C. Braitenberg^c, P. Fabris^b, B. Grillo^c

^a Centro Nazionale Terremoti, Istituto Nazionale di Geofisica e Vulcanologia, Roma, Italy

^b Centro Ricerche Sismologiche, Istituto Nazionale di Oceanografia e di Geofisica Sperimentale, Udine, Italy

^c Department of Mathematics and Geosciences, University of Trieste, Italy



Highlights

- Active slope deformation detected by GPS and tiltmeter stations in a karstic environment.
- We highlight a deformation pattern that is highly correlated with rainfall.
- A GPS dedicated measuring campaign characterizes the extension of the deformation.
- We characterize the recharge–discharge processes of the karst system.
- The observed slope deformation may have impact on the environmental risk evaluation.

UNCORRECTED PROOF

1
2
3
4
5
6
7
8
9
10
11
12
13
14
15
16
17
18
19
20
21
22
23
24
25
26
27
28
29
30
31
32
33
34
35
36
37
38
39
40
41
42
43
44
45
46
47
48
49
50
51
52
53
54
55
56
57
58
59
60
61
62
63
64
65
6667
68
69
70
71
72
73
74
75
76
77
78
79
80
81
82
83
84
85
86
87
88
89
90
91
92
93
94
95
96
97
98
99
100
101
102
103
104
105
106
107
108
109
110
111
112
113
114
115
116
117
118
119
120
121
122
123
124
125
126
127
128
129
130
131
132